PROCEEDINGS OF SPIE

SPIEDigitalLibrary.org/conference-proceedings-of-spie

Solar tracking using beam-steering lens arrays

Håkon J. D. Johnsen, Jan Torgersen, Astrid Aksnes

Håkon J. D. Johnsen, Jan Torgersen, Astrid Aksnes, "Solar tracking using beam-steering lens arrays," Proc. SPIE 10758, Nonimaging Optics: Efficient Design for Illumination and Solar Concentration XV, 1075805 (14 September 2018); doi: 10.1117/12.2320046

SPIE.

Event: SPIE Optical Engineering + Applications, 2018, San Diego, California, United States

Solar tracking using beam-steering lens arrays

Håkon J. D. Johnsen*[a], Jan Torgersen[a], and Astrid Aksnes[b]

[a]Department of Mechanical and Industrial Engineering, Norwegian University of Science and Technology, Trondheim, Norway
[b]Department of Electronic Systems, Norwegian University of Science and Technology, Trondheim, Norway

ABSTRACT

Conventional tracking solar concentrators track sunlight by rotating the concentrator optics to face the sun, which adds to the cost and bulk of the system. Beam-steering lens arrays, in contrast, allow solar tracking without bulk rotation of the optics. It consists of lens arrays stacked in an afocal configuration, and tracking is implemented by relative translation between these lens arrays. In this work, we present a phase-space methodology for analyzing and optimizing the performance of the beam-steering, and for revealing optical aberrations in the system. Using this methodology, we develop a beam-steering lens array with a simulated ≈70% efficiency across a two-axis ±40° tracking range, and a divergence of the outgoing beam of less than ±0.65°. We also present a functional small-scale prototype and demonstrate the feasibility of the concept for solar tracking. Beam-steering lens arrays can be placed in front of conventional concentrator optics and operated with little or no external tracking. This may enable low-cost robust concentrated solar power systems, and could also find other applications such as solar lighting and steerable illumination.

Keywords: beam-steering, lens arrays, solar tracking, micro-tracking, phase space

1. INTRODUCTION

Solar concentrators can provide highly concentrated solar power for applications such as concentrator photovoltaics, solar thermal energy, or solar lighting.[1] However, the concentrators require accurate solar tracking in order to achieve high concentration.[2] This tracking has traditionally been performed *external* to the concentrating optics, by mounting the concentrating optics to an external tracking system. The tracking system rotates the concentrating optics to keep it facing the sun, which introduces complicating factors including wind loads, the challenge of balancing the center of mass, and more complicated mechanical structures.[3]

As an alternative to external tracking, several studies[3–8] have recently considered *integrated* tracking, where an optical system tracks sunlight without being rotated towards the sun. Lin et al.[5] proposed a tracking-integrated beam-steering concept that emits collimated light, which can be used directly or passed on to a separate concentrator system as conceptually illustrated in Figure 1.

In this work, the beam-steering concept proposed by Lin et al is explored further, and we adopt the term beam-steering lens array (BSLA) for describing this type of concept.[†] First, the concept of BSLA for solar tracking is introduced, and discussed both from the perspective of paraxial optics and from the perspective of phase-space optics. Then, an optimization-based method is developed for designing BSLAs utilizing insights from phase-space optics. To demonstrate the feasibility of BSLA for large-range two-axis solar tracking, two different BSLA concepts are optimized using this design method. Finally, a physical proof-of-concept of a BSLA is presented.

* E-mail: hakon.j.d.johnsen@ntnu.no

[†]Related beam-steering concepts based on decentered lens arrays have previously been described using several different terms, including "beam steering with decentered microlens arrays",[9] "beam-deflecting microlens array telescopes",[10] "beam-scanning MLA system",[11] and "beam-steering array optics".[5] In this work, we choose to use "beam-steering lens arrays" (BSLA) as a general descriptive term for the concept of using decentered lens arrays for beam-steering.

Nonimaging Optics: Efficient Design for Illumination and Solar Concentration XV,
edited by Roland Winston, Eli Yablonovitch, Proc. of SPIE Vol. 10758, 1075805
 · doi: 10.1117/12.2320046

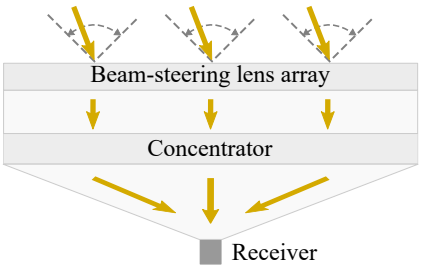

Figure 1: Conceptual illustration of how a beam-steering lens array can be combined with conventional concentrator optics.

2. BEAM-STEERING LENS ARRAYS

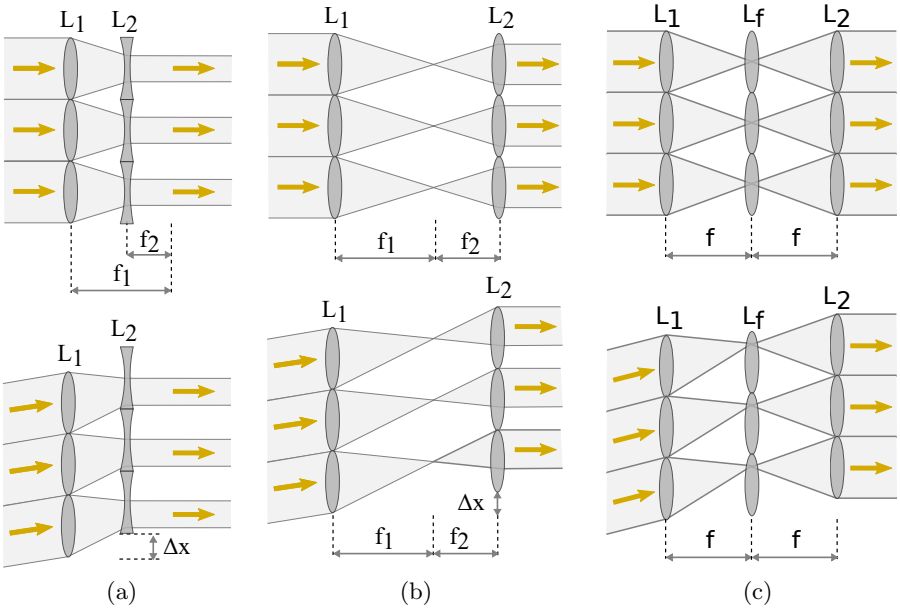

Figure 2: Paraxial beam-steering lens array principle using (a) Galilean configuration, (b) Keplerian configuration, and (c) Keplerian configuration including a field lens.

A basic BSLA consists of a pair of lens arrays arranged in an afocal configuration, allowing beam-steering by relative lateral translation of the two lens arrays as illustrated in Figure 2. This concept has previously been proposed for steering of laser beams.[9,11] Despite utilizing the same idea, there are some important differences between these laser applications and applications for solar energy:

- For laser beam-steering, a BSLA receives a beam parallel to its optical axis and emits it at an angle. For solar energy applications, the BSLA must be operated in reverse, receiving a beam at an angle, and emitting it parallel to the optical axis, as first proposed by Lin et al.[5]
- When used for solar energy, the BSLA must be orders of magnitude larger than when used for laser beam steering. This naturally also leads to larger lenslets.
- The coherence of laser light means that additional optics are required in order to allow for continuous laser beam steering.[11] This is not necessary for solar tracking, due to the reduced coherence of sunlight.

- The beam-steering range for laser beam-steering is typically on the order of 5° to 15°.[11–13] For solar tracking, much larger beam-steering angles are required.

Because of the large differences from previous laser applications, there is a need to re-think the concept and develop new design methods, which is the target of this work.

The idea behind this approach to beam-steering can be described both from the perspective of paraxial optics and from the perspective of phase-space optics.

2.1 Paraxial optics

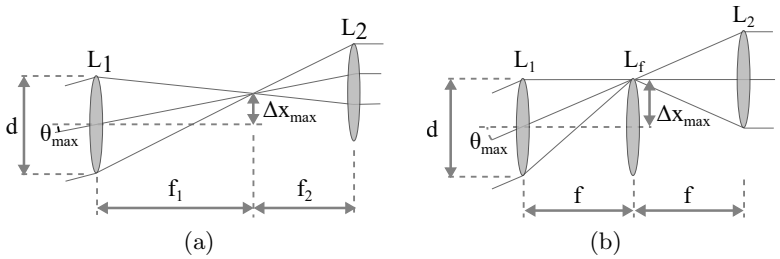

Figure 3: Geometry of a BSLA lenslet (a) without and (b) with a field lens, at maximum steering angle.

Figure 2a and Figure 2b show basic beam-steering lens arrays in Keplerian and Galilean configurations. The lens arrays are separated by their combined focal lengths $f_1 + f_2$. The BSLA can track incoming sunlight at an incidence angle θ by translating the last lens array a distance Δx such that the second lens array is always aligned with the focused image of the sun from the first lens array:

$$\Delta x \quad = \quad f_1 \cdot \tan\theta. \tag{1}$$

In order for all rays to reach the correct lens in the array L_2, the second focal length must be smaller than the first, as illustrated in Figure 3a. This leads to an angular magnification factor M:

$$M = \frac{f_1}{f_2} \quad = \quad 1 + 2\frac{f_1}{d}\tan\theta_{max}. \tag{2}$$

Sunlight has an inherent divergence of $\pm 0.27°$.[14] In order to limit the increase of divergence behind the BSLA and allow concentrators with high concentration factors, it is desirable that the angular magnification of the system is low. With two paraxial lenses, we therefore face a trade-off between the tracking range θ_{max}, and the additional divergence caused by angular magnification.

One approach to reduce this angular magnification is to add a field lens L_f to the BSLA in the Keplerian configuration, as shown in Figure 2c. With this approach, identical focal lengths f and an angular magnification of unity can be achieved.[9] However, with a field lens, the maximum tracking angle is limited to $\theta_{max} = \arctan\frac{d}{2f}$ as illustrated in Figure 3b.

2.2 Phase-space optics

A phase-space approach can be used to develop visual insight into the behavior and performance of a BSLA, and provides understandings that are useful in reducing the complexity of the design of such a system.

The trajectory of a ray in a geometrical optical system is determined by its position and direction. These parameters can be represented together in optical phase space, a space consisting of the linear dimensions as well as direction cosines of the optical ray. Phase-space optics is used to prove a number of important results in nonimaging optics,[2] and is also useful in visualizing the performance and aberrations of optical systems.[15]

For three-dimensional systems, four parameters are required to describe a ray-bundle crossing a surface - two directional parameters and two physical parameters. The phase-space representation of a three-dimensional optical system is therefore not very easy to visualize. However, much information about the system can be extracted from the two-dimensional counterpart, where ray-bundles crossing a surface can be described using only two parameters.[15]

Figure 4 shows the optical behavior of a paraxial BSLA from a phase-space perspective. At each indicated surface, ray-bundles from the whole tracking range are plotted in two-dimensional phase-space with their position x, and direction $p = n \cdot \sin\theta$. This illustrates the different transformations performed by the system: The lenses are used to convert a collimated beam with an angular offset into a focused ray-bundle with translational offset. This focused ray-bundle can then easily be tracked mechanically before being transformed back into a collimated beam.

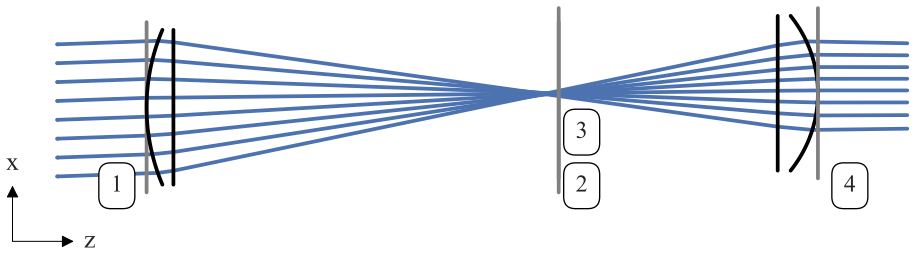

(a)

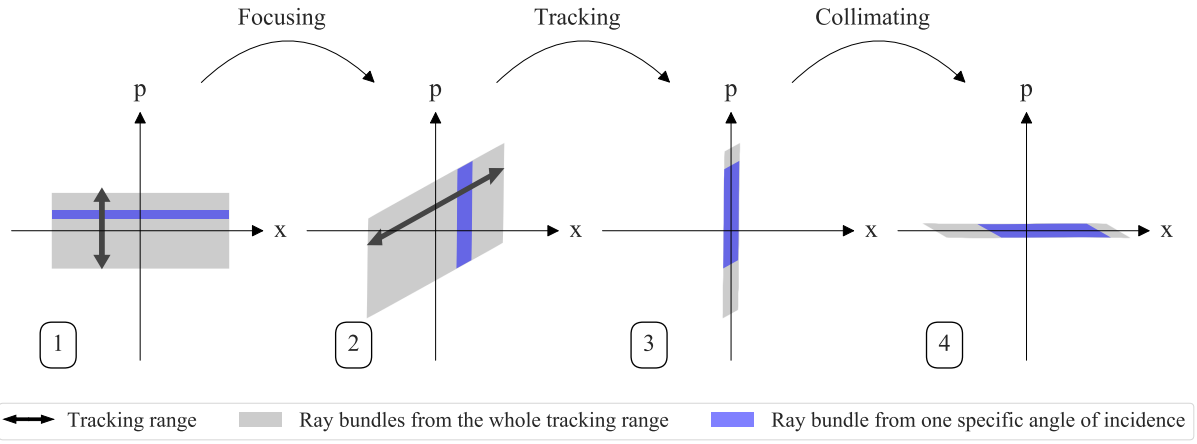

(b)

Figure 4: (a) Simple two-dimensional BSLA without field lens. (b) Sketch of the phase-space transformations performed by a two-dimensional paraxial BSLA. An incoming collimated ray bundle has a certain offset in direction p. The focusing lens transforms the rays into a focused bundle with a certain offset in position x. The tracker performs a coordinate transformation to center this position. Finally, the collimating lens transforms the rays into a centered collimated beam.

Figure 4 indicates that the phase-space transformation performed by the focusing lens has very different requirements from the phase-space transformation performed by the collimating lens:

- The focusing transformation is heavily overdetermined. From each separate tracking angle, the focusing lens should transform the incoming ray-bundle into a ray-bundle with a consistent phase-space geometry. The design problem is therefore very similar to design problems in conventional imaging optics, with one

important relaxation: the focused wavefronts should be *consistent*, but not necessarily *spherical*. This difference is further discussed and illustrated below.

- The collimating transformation should transform a single ray-bundle into a narrow collimated ray-bundle. This is a variant of the bundle-coupling problem of Nonimaging Optics, and well known design methods such as the Simultaneous Multiple Surface (SMS) method can give optimal or close to optimal solutions to this problem.[2]

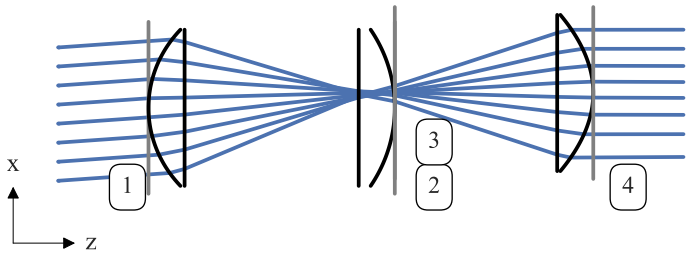

(a)

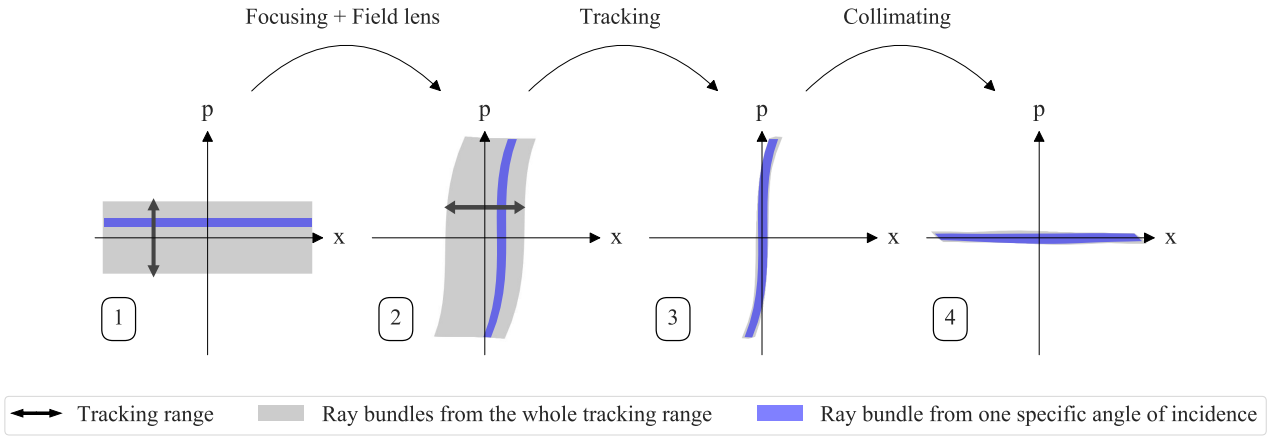

(b)

Figure 5: (a) Simple two-dimensional BSLA with field lens. (b) Phase-space transformations by this BSLA. The two first lenses are spherical, which is visible in the spherical aberration at surface 2 and 3. This spherical aberration is corrected by the final lens, which is aspherical.

Figure 5 shows phase-space plots of a real BSLA with a field lens, illustrating the difference between the focusing (and field) lens in a BSLA and a conventional imaging system. For illustration purposes, the focusing and field lenses in this system are spherical, leading to significant spherical aberration. This spherical aberration is visible as curved shapes in the second and third phase-space plots of Figure 5, and the lenses would therefore work poorly as an imaging system. As part of a BSLA however, the collimating lens is able to compensate for the spherical aberration. This is the major distinction between an imaging lens and the focusing lens in a BSLA: The performance of an imaging system depends on how well rays from a single field of the input, p, are mapped onto a position, x. In other words, it depends on the edges to be vertical in phase-space plot 2 of Figure 5. The performance of a BSLA on the other hand, does not require focusing to a perfect point. Instead, performance depends on the size of the total phase-space area to be collimated by the collimating lens. This area can be reduced by making ray-bundles from all the different incidence angles overlap as much as possible after tracking, as they do in phase-space plot 3 of Figure 5.

It is possible to estimate the performance of a BSLA directly without its collimating lens, by utilizing the properties of the phase-space transformations. Assuming that the collimating transformation can be solved with close to optimal performance, BSLA-performance can be predicted by evaluating the total occupied area in phase-space by all ray-bundles after tracking. The evaluated area is the etèndue of the ray-bundles,[15] and assuming optimal etèndue-conserving collimation, this directly gives the etèndue and the divergence of the collimated beam. This concept will be used for subdividing and simplifying the optimization problem for designing a BSLA.

3. OPTIMIZATION OF BEAM-STEERING LENS ARRAY

An optimization approach is developed for designing a three-dimensional BSLA. Optimization methods are more computationally expensive and less stable than direct solution methods, but they have the benefit that they readily handle overdetermined problems with the complexities of real-world systems such as wavelength dependent effects and manufacturing constraints.

3.1 Practical considerations

In order to implement a BSLA with high efficiency over a large two-axis field of view, some modifications must be done to the basic principles in Figure 2:

- The field lens in Figure 2c improves performance, but limits the tracking range to $\theta_{max} = \arctan \frac{d}{f}$. It can either be removed, or it can be allowed to move as part of the tracking motion in order not to limit the system's tracking range.
- For wide field of view, field curvature becomes significant, and planar tracking is not sufficient. Tracking is therefore allowed to follow a curved trajectory.
- For tight packing in a lens array, close-packed hexagonal lenses are used instead of circular lenses.
- The wide field of view and limited number of optical surfaces introduce large aberrations, which are compensated for by using thick lenses and allowing each lens surface to have an aspherical profile.

3.2 Formulation of optimization problem

We will consider three main performance indicators for quantifying and evaluating the performance of a complete BSLA:

- Maximizing tracking range
- Maximizing efficiency
- Minimizing divergence

The design of a BSLA can be considered a multi-objective optimization problem, where a solution must be found that provides a reasonable trade-off between these three performance indicators. Improving one of these indicators can be done at the cost of lower performance in the other indicators. For example increasing the tracking range will increase the off-axis optical aberrations, leading to increased divergence of the outgoing rays. Increasing the efficiency on the other hand imposes additional constraints on the system, leaving fewer degrees of freedom for handling the optical aberrations and decreasing divergence. Multi-objective optimization algorithms can be used to find a set of Pareto optimal solutions for these types of problems,[16] quantifying these trade-offs and allowing the designer to make an informed choice among the set of solutions. However, in order to limit the scope of this work, the optimization problem is reduced to a single-objective optimization problem in the following way:

- A sum scalarization[16] is performed to combine the efficiency and divergence into a single objective function.
- The racking range is fixed to a single value. In the design examples in this work, the value of $\pm 40°$ is chosen as an example of a relatively wide tracking range.

A sum scalarization allows optimization using simpler single-objective optimization algorithms, and a solution to the scalarized problem is also a solution to the original multi-objective problem.[16] However, this approach has the drawback that it gives only a single solution and therefore no information about the trade-off between the different performance indicators. The result is the following optimization problem

$$\min f(\mathbf{x}) = \sum_{i=1}^{m} \left(w_1 \frac{1}{\eta_i(\mathbf{x})} + w_2 \left(\delta\theta_i(\mathbf{x})\right)^2 \right) \tag{3}$$

$$\text{such that } g_j(\mathbf{x}) \leq 0 \tag{4}$$

where w_1 and w_2 are relative weights applied to the efficiency and divergence. $\eta_i(\mathbf{x})$ is the simulated efficiency for a ray-traced grid of rays with incidence angle number i and optical system described by $\mathbf{x}$. $\delta\theta_i(\mathbf{x})$ is the corresponding RMS divergence half-angle for field number i. m separate incidence angles are evaluated across the tracking range of the BSLA. $g_j(\mathbf{x})$ is a set of inequality constraints ensuring manufacturability, such as minimum and maximum thickness, and maximum lens curvature.

3.2.1 Separation of optimization procedure using phase-space optics

The optimization problem in Equations 3 and 4 can in theory be solved directly for the complete system, using ray-tracing simulations and a suitable optimization algorithm. However, it is a non-linear non-convex optimization problem with many variables, with no guarantee of finding the global minimum.

In order to reduce the complexity of the optimization problem and to increase the chance of finding a global minimum, the phase-space analysis from Section 2.2 can be utilized to subdivide the optimization problem. This gives the following final design process:

1. *Optimize focusing lens (and field lens, if included).* The optimization problem in Equations 3 and 4 is solved. $\eta_i(\mathbf{x})$ and $\delta\theta_i(\mathbf{x})$ are estimated by evaluating the volume in phase-space occupied by the set of bundles focused by the focusing (and field) lens. $\mathbf{x}$ contains only parameters varying the geometry of the focusing (and field) lens. The analysis in Section 2.2 considered only two-dimensional systems, but this volume estimate is readily extended to three-dimensional systems by assuming rotational symmetry of the collimating lens.

2. *Optimize a collimating lens for the optimized focusing lens.* The same optimization problem in Equations 3 and 4 is solved, but now $\eta_i(\mathbf{x})$ and $\delta\theta_i(\mathbf{x})$ are evaluated directly from ray-tracing results of the complete system, and $\mathbf{x}$ contains only parameters for the geometry of the collimating lens. This step might also be performed using a direct method such as the SMS method, bypassing the need for optimization in this step.

3. *Refine the complete system* by performing an optimization step where $\mathbf{x}$ contains all parameters for the complete system. This allows for any final improvements that were not achieved when optimizing separately due to inaccuracies in the phase-space model. For instance, the phase-space evaluation assumes a rotationally symmetric system, while the lenses are actually hexagonal when closely packed in an array. Some small additional improvements can therefore be gained by this final optimization step, and step 1 and 2 can be considered as a way to get a good initial starting point for this final optimization step.

4. DESIGN EXAMPLE

4.1 Methods

Two different systems were optimized using the optimization procedure outlined in Sections 3.2 & 3.2.1.

- One BSLA with three lens arrays: A focusing lens, a movable field lens, and a collimating lens. This was chosen in order to demonstrate how the benefits of a field lens can be extended to large tracking ranges when the field lens is allowed to move.

- One BSLA with only two lens arrays: A focusing lens and a collimating lens. This was chosen in order to demonstrate a BSLA without the mechanical complexity of the movable field lens.

Both BSLAs were simulated across the AM1.5D solar spectrum,[17] with Poly(methyl methacrylate) (PMMA) as lens material, using a custom sequential three-dimensional ray-tracer. The ray-tracer was written in Python and accelerated using Numba.[18] Optimization was performed using a combination of the Differential Evolution, Basinhopping and L-BFGS-B-algorithms available from SciPy.[19]

Table 1: Constraints used in optimization of BSLA. The dimensions of the system are scalable with the arbitrary scaling factor k.

Parameter	Constraint
Semi-diameter of lenses	$1.0 \cdot k$
Minimum thickness at thinnest point of lens	$0.5 \cdot k$
Maximum thickness at thickest point of lens	$2.0 \cdot k$
Minimum air gap between lenses	$0.05 \cdot k$
Maximum air gap between lenses	$2.0 \cdot k$
Minimum radius of curvature on lens	$0.7 \cdot k$
Maximum aspect ratio of single surface	0.5

Fresnel reflections and dispersion were taken into account, while material absorption was ignored*. Hexagonal lenses were used for all simulations to allow for close packing in a lens array. The divergence of outgoing light was estimated as a combination of divergence due to optical aberrations, and divergence due to magnification of the inherent divergence of sunlight.

The constraints from Table 1 were used to ensure reasonable, manufacturable designs. For the design with a field lens, the lateral translation of the two lens arrays were constrained to be proportional to each other, allowing linked control sharing the same mechanical actuator.

Plots of efficiency and divergence half-angle are created using ray-tracing of 80 000 random rays per incidence angle, with random wavelengths according to the AM1.5D spectrum and random directions within the 0.27° divergence half-angle of sunlight. The plotted divergence half-angle is defined as the half-angle encircling 90% of the transmitted energy. The plotted efficiency takes into account Fresnel reflections, but does not consider material absorption or cosine projection loss.

4.2 Results and discussion

The resulting optimized design with a field lens is shown in Figure 6a, and the system without a field lens is shown in Figure 6b. The simulated optical performance under solar irradiation is shown in Figure 7. The system with a field lens has lower optical efficiency at low angles of incidence, due to the increased number of optical surfaces. However, at high incidence angles, it still surpasses the efficiency of the system without a field lens.

The additional divergence introduced by the BSLA requires the use of concentrator optics with higher acceptance angle, decreasing the maximum achievable concentration ratio. However, the results in Figure 7 show that by including a field lens, this final divergence half-angle can be kept at less than 0.65° across the tracking range, which will still permit approximately 7800x concentration from an ideal concentrator.[2]

With increased angle of incidence, intensity of sunlight received by a flat stationary receiver decreases due to the cosine projection effect. Even if the lens design is improved with a higher acceptance angle, power will therefore be low for high angles of incidence, and some amount of external tracking might be required for

*Material absorption depends on the physical dimensions of the BSLA, which are not fixed in these design examples

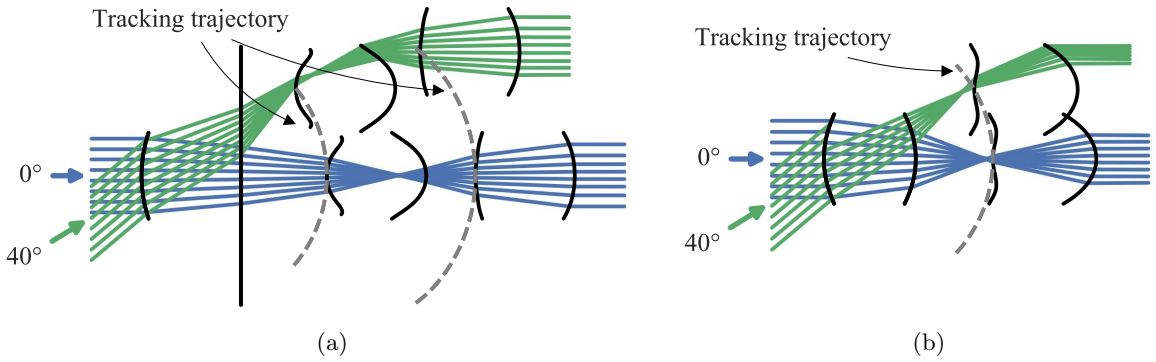

Figure 6: Ray-traced sketch of optimized system (a) with, and (b) without field lens.

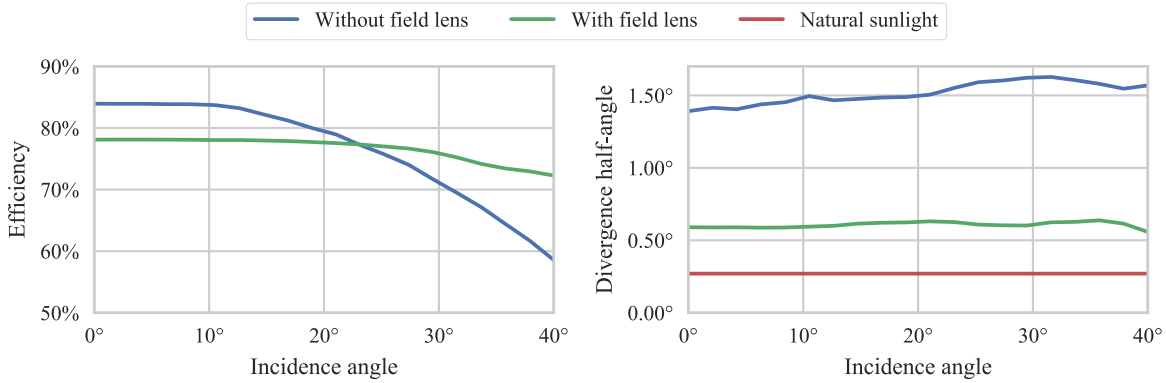

Figure 7: Simulated optical performance with and without field lens. Using a field lens reduces divergence significantly at the cost of increased mechanical complexity. Inherent divergence of natural sunlight is included for reference.

efficient full-day operation. Yet, we conclude that the use of beam-steering lens arrays still significantly reduces the requirements for this external tracking.

Figure 8 shows two-dimensional phase-space plots of the optimized systems. The phase-space plots are generated at the focal point after tracking. As discussed in Section 2.2, performance of the focusing transformation depends on how well the ray-bundles from one specific wavelength and angle of incidence overlap with all other ray bundles. For the BSLA without field lens (Figure 8b) we can see that the optimization algorithm has chosen a focusing lens where the shape of the total occupied area in phase-space is strongly nonlinear, but this is not a problem for the collimating lens. We can also see that ray-bundles from different wavelengths don't overlap very well, indicating significant chromatic aberration. For the BSLA with field lens, in Figure 8a, we see that the field lens is able to significantly improve the overlap of the ray-bundles, especially the overlap in momentum. In addition, the ray-bundles for different wavelengths overlap more. This leads to the reduced divergence after collimation and improved performance.

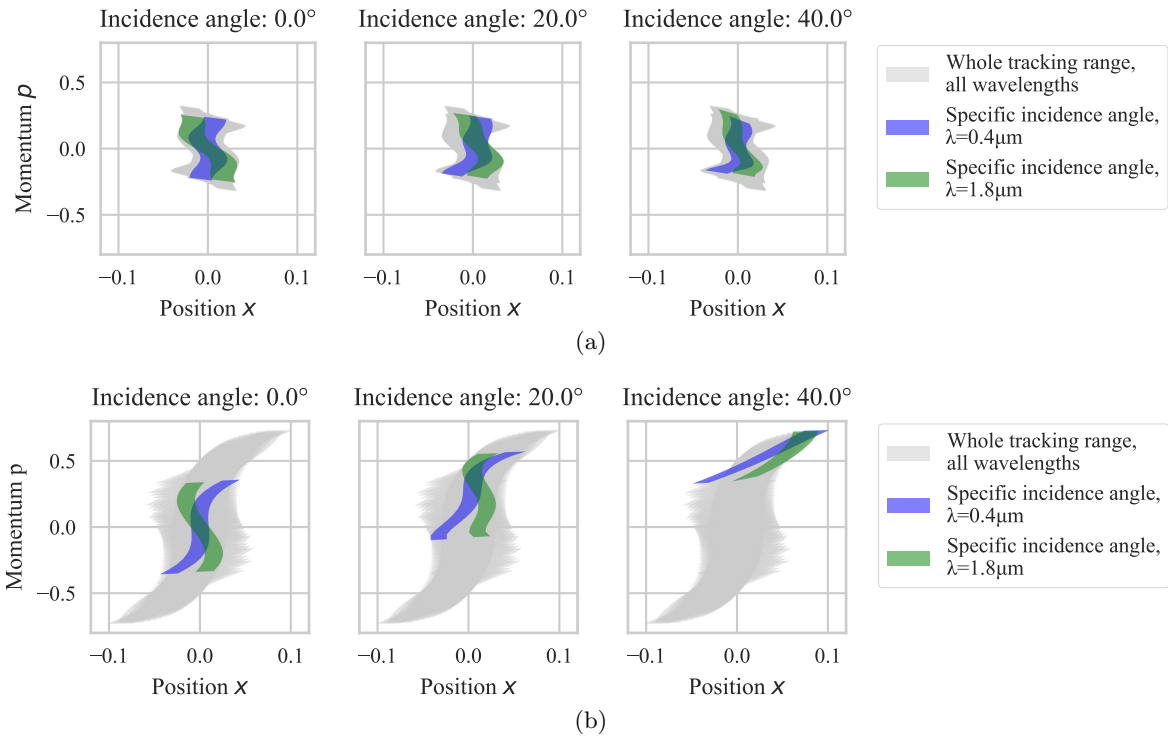

Figure 8: Two-dimensional phase-space plots at focal point. For system (a) with, and (b) without field lens.

5. PROOF-OF-CONCEPT

A physical and functional proof-of-concept with automatic tracking has been created using a previously optimized BSLA design. The design was created using an earlier optimization technique, with lower performance.[20] Despite this lower performance, the proof-of-concept serves to demonstrate the feasibility of creating a complete, functional BSLA. As an example use case for this proof-of-concept, the BSLA has been attached to an off-axis parabolic reflector that illuminates a target from the underside. This specific configuration is a scaled-down version of a solar cooking concept using BSLA.

5.1 Manufacturing and testing methods

Compression molds for the lens arrays were machined in aluminum on an in-house Computer Numerical Control (CNC) milling machine, due to the lack of access to high-precision optical manufacturing equipment. These molds were used for compression molding of PMMA plates.

The tracking motion is actuated using SG-92R micro servos and controlled from an Arduino Nano development board. The system uses a combination of open- and closed-loop control, and both control loops have been implemented with low-cost photocells: Approximate solar position is detected using a set of four inclined photocells, each inclined ±40° from the front plane about their respective axes. The four photocells sense different relative brightness values due to their different angle towards the sun and the cosine projection loss. From this data, the incidence angle of the sunlight can be inferred. The microcontroller orients the BSLA to this approximate angle. Secondly, the tracking is fine-tuned by diverting a small section of the input aperture to a set of photocells that measure tracking error, and a closed control loop is implemented in order to minimize this tracking error.

An image analysis setup was used for testing the optical performance of the completed BSLA, as reported in earlier work.[20]

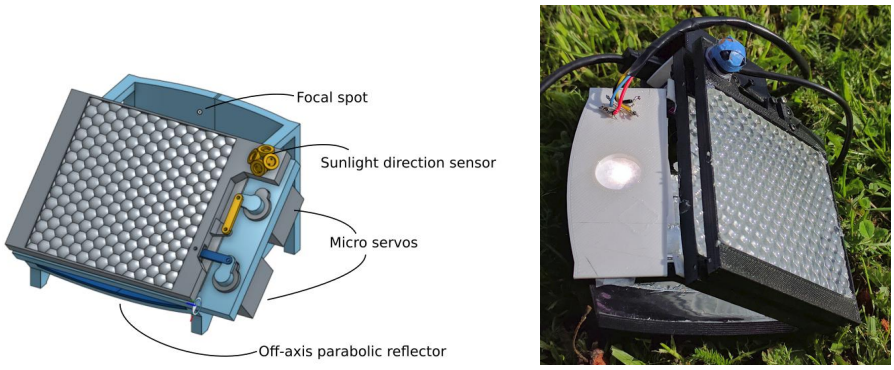

(a) (b)

Figure 9: (a) 3D model of Proof-of-concept with concentrator (b) Video of proof-of-concept tested outside in the sun. http://dx.doi.org/10.1117/12.2320046.1

5.2 Results

A 3D model of the proof-of-concept attached to a concentrator is shown in Figure 9a, and the device is shown outside in the sun in Figure 9b.

Figure 10 shows the measured optical performance of the proof-of-concept BSLA, compared to simulated values. The results show ≈ 10% reduced efficiency compared to the simulated values, and approximately a doubling of divergence compared to simulation. The high divergence is likely a result of a waviness in the surface of the lens array, due to the low precision of the mold manufacturing process. With improved mold manufacturing and corresponding increased surface quality, future prototypes are expected to better follow the predicted performance.

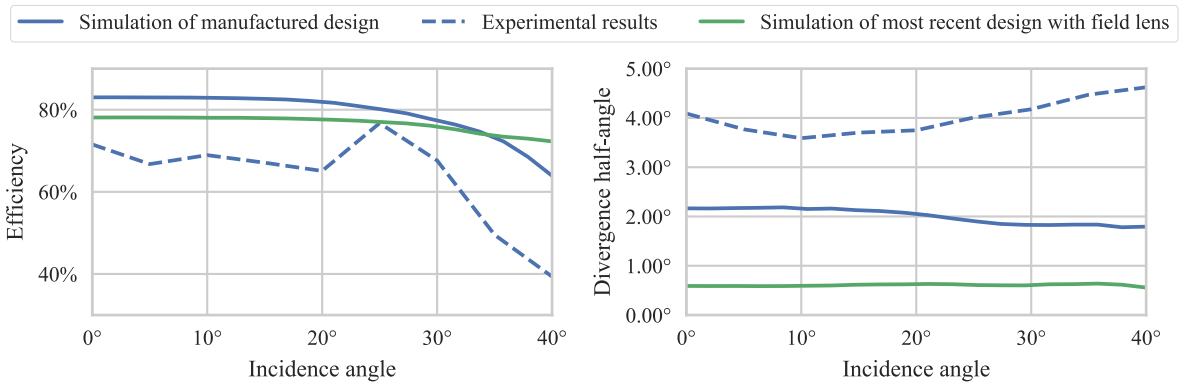

Figure 10: Simulated and measured efficiency and divergence of the proof-of-concept over its field of view.

6. OUTLOOK AND CONCLUSIONS

We have shown that beam-steering lens arrays can be used to track and redirect sunlight with low losses over a two-axis ±40˚ tracking range, and we have presented an optimization-based design method for designing such systems. We have also demonstrated a physical proof-of-concept, demonstrating its practicality in the real world. Further work will involve exploration of the solution space, by mapping the trade-off between tracking range, efficiency, and divergence, as well as the impact of the selected manufacturing constraints. We are also planning to create a new proof-of-concept according to updated BSLA designs, and with improved manufacturing methods.

Beam-steering lens arrays can be made from common low-cost materials such as PMMA, and they can be compatible with high-volume production techniques such as injection molding or hot embossing. They may therefore foster the development of low-cost, small-scale solar energy systems for a number of applications including solar cooking, small-scale solar thermal processing, solar water heating, concentrator photovoltaics and solar lighting.

REFERENCES

[1] Xie, W. T., Dai, Y. J., Wang, R. Z., and Sumathy, K., "Concentrated solar energy applications using Fresnel lenses: A review," *Renewable and Sustainable Energy Reviews* **15**, 2588–2606 (Aug. 2011).

[2] Winston, R., Minano, J. C., Benitez, P. G., contributions by Narkis Shatz and John C. Bortz, W., and Bortz, J. C., [*Nonimaging Optics*], Saint Louis : Elsevier Science, Saint Louis (2005).

[3] Apostoleris, H., Stefancich, M., and Chiesa, M., "Tracking-integrated systems for concentrating photovoltaics," *Nature Energy* **1**, 16018 (Mar. 2016).

[4] Grede, A. J., Price, J. S., and Giebink, N. C., "Fundamental and practical limits of planar tracking solar concentrators," *Optics Express* **24**, A1635–A1646 (Dec. 2016).

[5] Lin, W., Benitez, P., and Miñano, J. C., "Beam-steering array optics designs with the SMS method," *Proc. SPIE* **8485**, 848505–848505–7 (2012).

[6] Campbell, R. and Machado, M., "LOW cost CPV = Embedded CPV with internal tracker," in [*2010 35th IEEE Photovoltaic Specialists Conference (PVSC)*], 003003–003007 (June 2010).

[7] Duerr, F., Meuret, Y., and Thienpont, H., "Tailored free-form optics with movement to integrate tracking in concentrating photovoltaics," *Optics Express* **21**, A401–A411 (May 2013).

[8] Hallas, J. M., Baker, K. A., Karp, J. H., Tremblay, E. J., and Ford, J. E., "Two-axis solar tracking accomplished through small lateral translations," *Applied Optics* **51**, 6117 (Sept. 2012).

[9] Watson, E. A., "Analysis of beam steering with decentered microlens arrays," *Optical Engineering* **32**(11), 2665–2670 (1993).

[10] Duparré, J., Radtke, D., and Dannberg, P., "Implementation of field lens arrays in beam-deflecting microlens array telescopes," *Applied Optics* **43**, 4854–4861 (Sept. 2004).

[11] Akatay, A., Ataman, C., and Urey, H., "High-resolution beam steering using microlens arrays," *Optics Letters* **31**, 2861–2863 (Oct. 2006).

[12] Bourderionnet, J., Rungenhagen, M., Dolfi, D., and Tholl, H. D., "Continuous laser beam steering with micro-optical arrays: Experimental results," *Proc. SPIE* **7113**, 71130Z, International Society for Optics and Photonics (Oct. 2008).

[13] Xiang, J., Wu, N., Zhang, J., and Wu, L., "Design of driving and control system based on Voice Coil Actuation for linear motion of micro-lens array," *Proc. SPIE* **7133**, 713330, International Society for Optics and Photonics (Jan. 2009).

[14] Kalogirou, S. A., [*Solar Energy Engineering: Processes and Systems*], Academic Press (Oct. 2013).

[15] Herkommer, A. M., "Phase space optics: An alternate approach to freeform optical systems," *Proc. SPIE* **53**, 031304 (Dec. 2013).

[16] Pardalos, P. M., Žilinskas, A., and Žilinskas, J., [*Non-Convex Multi-Objective Optimization*], Springer Optimization and Its Applications, Springer International Publishing (2017).

[17] Renewable Resource Data Center, "Solar Spectral Irradiance: Air Mass 1.5." https://rredc.nrel.gov/solar/spectra/am1.5/.

[18] Lam, S. K., Pitrou, A., and Seibert, S., "Numba: A LLVM-based Python JIT Compiler," in [*Proceedings of the Second Workshop on the LLVM Compiler Infrastructure in HPC*], *LLVM '15*, 7:1–7:6, ACM, New York, NY, USA (2015).

[19] Jones, E., Oliphant, T., Peterson, P., and others, "SciPy: Open source scientific tools for Python," (2001).

[20] Johnsen, H. J. D., "Novel Low Cost Solar Thermal Energy Concepts for Developing Countries," *NTNU* (2017).